Title
Mass and Density of the B-Type Asteroid (702) Alauda

Journal
The Astrophysical Journal, 727(2)

ISSN
0004-637X 1538-4357

Authors
Rojo, P.
Margot, J.L.

Publication Date
2011-02-01

DOI
10.1088/0004-637X/727/2/69

Peer reviewed

DRAFT VERSION NOVEMBER 30, 2010
Preprint typeset using LaTeX style emulateapj v. 8/13/10

MASS AND DENSITY OF B-TYPE ASTEROID (702) ALAUDA

P. ROJO
Departamento de Astronomia
Universidad de Chile
Santiago, Chile

J. L. MARGOT
Departments of Earth and Space Sciences, Physics and Astronomy
University of California, Los Angeles
Los Angeles, CA 90095

Draft version November 30, 2010

ABSTRACT

Observations with the adaptive optics system on the Very Large Telescope reveal that outer main belt asteroid (702) Alauda has a small satellite with primary to secondary diameter ratio of $\sim$56. The secondary revolves around the primary in 4.9143 $\pm$ 0.007 days at a distance of 1227 $\pm$ 24 km, yielding a total system mass of (6.057 $\pm$ 0.36) $\times$ 10^{18} kg. Combined with an IRAS size measurement, our data yield a bulk density for this B-type asteroid of 1570 $\pm$ 500 kg m^{-3}.

Subject headings: Astrometry; Ephemerides; Instrumentation: adaptive optics; Minor planets, asteroids: individual: 702 Alauda; Minor planets, asteroids: general; Techniques: high angular resolution

1. INTRODUCTION

The discovery of solar system binaries has a considerable impact on key problems in planetary science, partly because the binaries allow direct measurements of fundamental physical and chemical properties that are otherwise only obtainable with spacecraft. Characteristics of the mutual orbit provide crucial information about asteroid bulk properties and internal structure, such as mass, density, porosity, and mechanical strength. These measurements are used to establish links between asteroids and meteorites, and to understand the geological context of meteorites that can be studied in great detail in the laboratory. Density measurements can also constrain the proportion of ice to rock in distant minor planets, which is a strong indicator of the chemical environment at the time of formation (Lunine and Tittemore 1993; Johnson and Lunine 2005). The current proportion of binary systems and their configuration are strong tracers of the collisional and dynamical evolution of small bodies in the solar system. Binaries therefore illuminate the conditions in the solar nebula and early solar system, and they help us refine our understanding of planet formation. The very high science priority of characterizing binary systems has been reviewed by Weidenschilling et al. (1989); Merline et al. (2002); Margot (2002); Burns (2002); Noll et al. (2008).

The third largest asteroid and former planet (2) Pallas (a=2.772 AU, e=0.231, i=34.8°) belongs to the taxonomic class B, which is characterized by a linear featureless spectrum with bluish to neutral slope in the wavelength range (0.435-0.925 μm) (Bus and Binzel 2002). In the case of Pallas, a broad absorption band in the 3 μm region is detected (Larson et al. 1983; Jones et al. 1990) suggestive of hydrothermal alteration and reminiscent of carbonaceous chondrite material (Sato et al. 1997). The negative spectral slope of B-type asteroids is attributed by Yang and Jewitt (2010) to a broad absorption band near 1.0 μm. Because B-type asteroids may represent relatively primitive material with similarities to carbonaceous meteorites (Larson et al. 1983; Sato et al. 1997; Yang and Jewitt 2010), their characterization can further our understanding of the primordial building blocks of planets. Unfortunately, our knowledge of the density of B-type asteroids is poor, in part because few measurements exist, and in part because mass estimates for (2) Pallas are widely scattered as they rely on indirect techniques (gravitational perturbations on other asteroids or Mars). Carry et al. (2010) reported a density of 3400 $\pm$ 900 kg m^{-3} based on a mass estimate derived from pertubations to the orbits of asteroids (Michalak 2000) with 22% uncertainties and their volume estimate with 4% uncertainties. Schmidt et al. (2009) reported a density of 2400 $\pm$ 250 kg m^{-3} based on a mass estimate derived from perturbations to the orbit of Mars (Konopliv et al. 2006) with 2.7% uncertainties and their volume estimate with 10% uncertainties. However their report lists mass estimates for Pallas that vary by 20%, and a more extensive survey indicates mass estimates that vary by 60% (Hilton 2002). Using the mass estimates of Hilton (1999) and Michalak (2000) and the volume of (Schmidt et al. 2009) yields densities for Pallas in the range of 3700 $\pm$ 390 kg m^{-3} and 2800 $\pm$ 670 kg m^{-3}, respectively. Here we report on the discovery (Rojo and Margot 2007) and tracking of the first satellite to a B-type asteroid, (702) Alauda (a=3.191 AU, e=0.022, i=20.6°), which allows us to provide a direct mass measurement and improved density estimates for this class of asteroids.

(702) Alauda has been identified as the largest member of a highly inclined dynamical family in the outer main belt of asteroids (Foglia and Masi 2004; Gil-Hutton 2006). It is reasonable to assume that the creation of this binary system dates back to the impact responsible for the formation of the family (Michel et al. 2001; Durda et al. 2004). Because tidal evolution depends on the formation age of the binary and the mechanical properties of the components, our observations can also be used to provide a relationship between formation age and mechanical strength, specifically shear modulus and tidal dissipation factor (Taylor and Margot 2010).

Electronic address: pato@das.uchile.cl
Electronic address: jlm@astro.ucla.edu

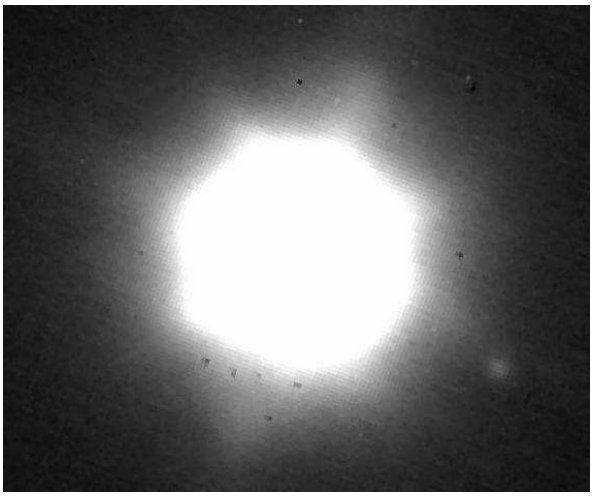

Figure 1. H-band image of the (702) Alauda binary system. The companion is clearly seen in the lower-right quadrant.

2. OBSERVATIONS AND DATA REDUCTION

Using a highly optimized observing strategy, we were able to observe a total of 111 unique main belt and Trojan asteroids during three nights in visitor mode at the Very Large Telescope (VLT). We used the adaptive optics (AO) instrument NaCo (Lenzen et al. 2003; Rousset et al. 2003) that has an 1024x1024 pixel InSb array detector, which is fed by an adaptive optics system consisting on Shack-Hartmann sensor with a 14x14 lenslet array. Information from the wavefront sensor is used to control both a tip-tilt mirror and a deformable mirror. We used NaCo in its S13 mode, resulting in a pixel scale of 13.72 mas.

The observing sequence for each target consisted of four 10-second integrations in each of four different offset positions. Each frame was then flat-fielded, and subtracted in pairs to remove the sky, before alignment and addition to form a composite image. We also obtained a bad-pixel mask from outlier pixels present in the averaged flat-field, and used the mask to ignore those pixels in each of the 10-second frame.

The companion to (702) Alauda was identified in a 40-second composite image in the Ks filter ($\lambda_c = 2.18\mu$m, FWHM $= 0.35\mu$m). We eliminated the possibility of one type of AO artifact (a non-rotating waffle mode) by immediately performing an observing sequence with the field of view rotated 50 degrees. The non-sidereal tracking of the telescope discarded fixed background sources and most moving background sources. Follow-up observations that night and the next fully confirmed the binarity of the system.

The binary system was observed at 6 epochs during the last 2 nights of the observing run with different filters. The H-filter ($\lambda_c = 1.66\mu$m, FWHM $= 0.33\mu$m) was found to give the best compromise between SNR and AO correction (Fig. 1). In order to secure additional astrometric measurements, we submitted a Director's Discretionary Time (DDT) proposal to follow-up the system in queue mode, using the same observing instrument and strategy. Table 1 summarizes all the observations of the binary system.

We attempted to detect the companion in our composite images, and also in images where an azimuthally averaged profile was subtracted from the primary source. We obtained ten secure detections. The secondary may be undetectable in other images due to proximity to the primary, atmospheric seeing, lunar phase, or a combination of factors. We performed aperture photometry of the primary on the composite images, and of the secondary on the profile-subtracted images, removing a slanted-plane sky background where necessary. We then combined the primary and secondary photometry to measure primary-to-secondary flux ratios and relative positions.

Our orbit determination software uses the separation and position angle of the secondary with respect to the primary to solve for the orbital parameters in the two-body problem. The mutual orbital plane orientation is assumed constant, but heliocentric motions and light-time corrections are taken into account. Astrometric positions and their errors are specified at the mid-time of the exposure sequence. Starting from thousands of initial conditions, the software adjusts for seven parameters (equivalent to six orbital elements plus the mass of the system) in the nonlinear ordinary least squares problem with a Levenberg-Marquardt technique. The covariance matrix and post-fit residuals are computed and inspected. Binary orbits have been computed with this algorithm for near-Earth asteroids (Margot et al. 2002; Ostro et al. 2006), main-belt asteroids (Margot and Brown 2003; Merline et al. 2002), Kuiper belt objects (Noll et al. 2008; Petit et al. 2008), dwarf planets, and binary stars.

3. RESULTS

Primary-to-secondary flux ratios from the photometric analysis are shown in Fig. 2. Some, but not all, of the observed variations may be related to the rotation of the primary with period 8.3539 ± 0.0007 hrs and lightcurve amplitude of 0.09 ± 0.02 mag (Benishek 2008) or to the rotation of the secondary, which we expect to be spin-locked (tidal despinning timescale $\sim 10^6$ years). Considering the theoretical Poisson noise ($\lesssim 0.05$mag), the differences in the same-night ratio measurements for the J and H filters (0.21 and 0.27 magnitudes, respectively) must be attributed to unknown systematics. The average of the primary-to-secondary flux ratio is 3188 ± 1444 (magnitude difference of $8.8^{+0.4}_{-0.7}$), where the quoted uncertainty is the standard deviation of our measurements. This ratio is one of the largest for solar system binaries, although a satellite of (41) Daphne is reported to be 10 magnitudes fainter than the primary (Conrad et al. 2008). If we assume that the primary and secondary have similar albedoes, the primary-to-secondary diameter ratio is $\sim$56, and the mass of the secondary represents an insignificant fraction of the total mass budget.

Relative positions of the components at the epochs of our measurements are shown in Table 2. Since we only have one measurement per epoch, as an upper limit we assigned centering uncertainties of 0.013 arcseconds in x and y, equivalent to the plate scale of the detector.

Our 7-parameter orbital fits (Fig. 3) used 16 measurements at 8 epochs. The best-fit reduced chi-square value was 0.665, indicating that our uncertainties were assigned somewhat conservatively but not overly so. Values of the fitted parameters and their formal standard errors are shown in Table 3. We measure a system mass of $(6.057 \pm 0.36) \times 10^{18}$ kg (roughly 10^{-6} Earth masses), corresponding to a fractional precision of 6%, considerably better than results from indirect techniques.

The IRAS Minor Planet Survey (IMPS) lists the diameter of (702) Alauda as 194.73 $\pm$ 3.2 km. Combining our mass measurement with this size estimate, we compute a density with formal uncertainties of 1570 $\pm$ 120 kg m^{-3}. Realistic uncertainties need to take into account the fact that there may be a bias in the asteroid size and that the shape of the asteroid

UT Date and time	MJD	Filter	RA (deg)	DEC (deg)	Δ (AU)	Detection
2007 07 26 06:24	54307.2664	Ks	316.7047	-3.7504	2.1555	1
2007 07 26 07:26	54307.3098	H	316.6957	-3.7485	2.1554	1
2007 07 26 07:35	54307.3159	J	316.6942	-3.7482	2.1553	1
2007 07 26 07:46	54307.3235	H	316.6927	-3.7479	2.1553	1
2007 07 27 03:44	54308.1553	H	316.5163	-3.7124	2.1528	1
2007 07 27 05:58	54308.2486	H	316.4965	-3.7085	2.1526	1
2007 08 18 04:07	54330.1716	H	311.7363	-3.2049	2.1565	1
2007 08 29 04:12	54341.1750	H	309.6719	-3.2051	2.2082	0
2007 09 09 01:45	54352.0731	H	308.1241	-3.2997	2.2884	1
2007 09 10 02:45	54353.1147	H	308.0073	-3.3115	2.2974	0
2007 09 11 01:39	54354.0685	H	307.9053	-3.3225	2.3059	1
2007 09 12 04:09	54355.1727	H	307.7935	-3.3355	2.3159	0
2007 09 13 02:12	54356.0920	H	307.7056	-3.3464	2.3245	0
2007 09 14 01:46	54357.0738	H	307.6167	-3.3581	2.3338	1
2007 09 15 01:10	54358.0488	H	307.5338	-3.3698	2.3432	0
2007 09 16 02:18	54359.0959	H	307.4507	-3.3823	2.3535	0
2007 09 20 01:06	54363.0457	H	307.1929	-3.4286	2.3940	0
2007 09 21 00:54	54364.0377	H	307.1420	-3.4398	2.4046	0
2007 09 28 01:56	54371.0804	H	306.9412	-3.5097	2.4841	0
2007 09 30 03:32	54373.1471	H	306.9351	-3.5261	2.5086	0

Table 1
Observational circumstances. Times listed refer to the start of the third exposure, roughly the middle of the four-image exposure sequence. Observation epochs are given in Universal Time (UT) and Modified Julian Date (MJD) formats. The Right Ascension (RA), Declination (DEC) and geocentric distance (Δ) are used in orbital fits. Observations above and below the line were obtained in visitor and queue mode, respectively.

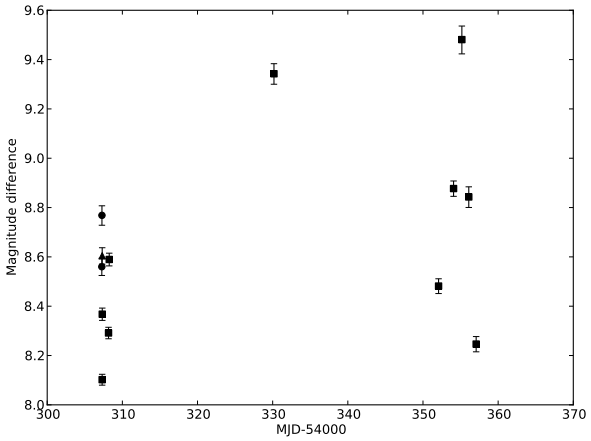

Figure 2. Primary-to-secondary magnitude differences for positive detections. Triangle, squares, and circles indicate the measurements using the J, H, and Ks filters, respectively. The error bars indicate the Poisson uncertainty.

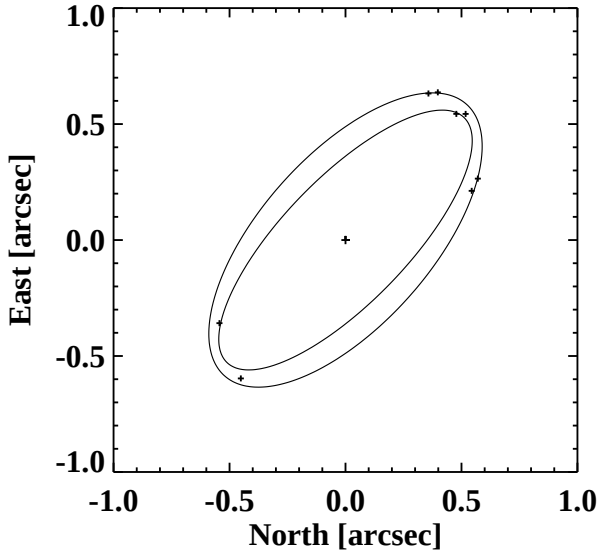

Figure 3. Observed secondary-to-primary separations and position angles, with error bars (crosses), and best-fit orbit (solid lines). The exterior ellipse shows the projection of the orbit on the plane of the sky (62 degree inclination) on MJD 54307; it is representative of the first four astrometry data points at position angles 21, 25, 58, and 60 degrees. The interior ellipse shows the projection of the best-fit orbit on the plane of the sky (69 degree inclination) fifty days later; it is more representative of the last three astrometry data points at position angles 46, 49 and 213 degrees.

may differ substantially from a sphere. The IMPS diameter measurements have been compared with occultation results and are believed to be accurate to 10% (Tedesco et al. 2002). Therefore we suggest a density estimate with more realistic errors of 1570 ± 500 kg m^{-3}.

The confounding effects of porosity must be kept in mind in interpreting density measurements (Britt et al. 2002; McKinnon et al. 2008). In Fig. 4 we show the range of grain densities that are compatible with our bulk density for several values of porosity. Because the pressure at the center of (702) Alauda is moderate ($\sim$3.3 MPa or $\sim$33 atmospheres), this body could in principle sustain fairly large porosities. At near-zero porosities a mix of anhydrous silicates and water ice would require a fair amount of ice (roughly 3/4 by volume or 4/9 by mass) to match the density constraint. At high porosities the asteroid could be entirely devoid of ice. Progress in fully understanding the manifestation of porosity in small bodies will require a large sample of reliable sizes and densities, or in-situ seismic experiments.

UT Date and time	MJD	Sep (asec)	PA (deg)	Res. (North)	Res. (East)
2007 07 26 06:24	54307.2663	0.584	21.3	0.975	0.588
2007 07 26 07:46	54307.3235	0.629	24.9	-0.081	-0.167
2007 07 27 03:44	54308.1553	0.751	58.0	0.942	-0.446
2007 07 27 05:58	54308.2486	0.726	60.5	-0.063	0.014
2007 08 18 04:07	54330.1716	0.748	232.9	-0.418	-1.165
2007 09 09 01:45	54352.0731	0.751	46.4	-0.924	-0.554
2007 09 11 01:39	54354.0685	0.651	213.4	0.530	0.357
2007 09 14 01:46	54357.0738	0.724	48.7	-0.640	-0.230

Table 2
Astrometry used in our orbital solution, showing the positions of the secondary relative to the primary, expressed as separations (Sep) in arcseconds and position angles (PA) in degrees East of North. Epochs are given as in Table 1. Also shown are residuals from our best-fit solution in the format (O-C)/σ.

Parameter		Estimate	$\sigma_{\rm formal}$
Orbital period [days]	P	4.9143	0.007
Semi-major axis [km]	a	1226.5	24
Eccentricity	e	0.003	0.02
Longitude of ascending node [deg]	Ω	280.9	3
Inclination [deg]	i	46.5	3
Argument of pericenter [deg]	ω	169.074	180
Epoch of pericenter passage [MJD]	T	54308.648	4

Table 3
Results of orbital fits to our astrometry, giving parameter estimates and formal standard errors. Angles are provided in the equatorial frame of epoch J2000. The orbit normal is at right ascension 190.9° and declination 43.5°, corresponding to ecliptic longitude 168.3° and latitude 43.3°. The orientation of pericenter and time of pericenter passage are poorly constrained, as expected for such a low eccentricity orbit. Nevertheless we provide guard digits in those quantities to allow computation of the relative positions of the components without loss of precision.

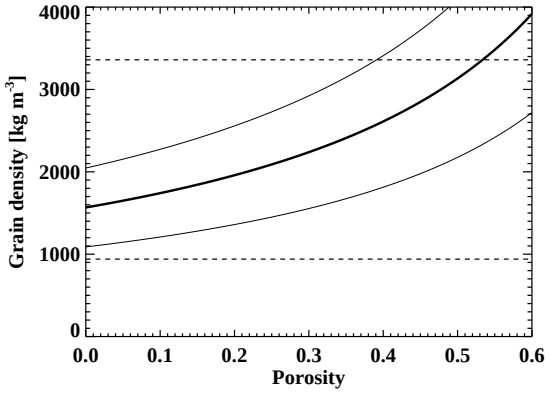

Figure 4. Range of porosities and grain densities admitted by our density measurement (our nominal solution is the bold solid line, with density uncertainties captured by the solid lines above and below). The densities of water ice and anhydrous silicates are shown as dashed lines.

4. CONCLUSIONS

We report the discovery of a satellite to (702) Alauda, a member of an asteroid collisional family. The satellite is small, with a ratio of primary to secondary radii of about 50. The secondary revolves around the primary in 4.91 days at a distance of 1,230 km, corresponding to 12.6 primary radii. Due to tidal interactions, its spin period is expected to synchronize to its orbital period on million year timescales. The secondary likely formed by a sub-catastrophic collision on the primary, and subsequently tidally evolved outward (Merline et al. 2002; Durda et al. 2004). Because the orbit is quasi-circular it is likely that the secondary is mechanically weaker than the primary (Margot and Brown 2003; Taylor and Margot 2010), as might be expected if the body formed by the re-accumulation of impact ejecta. Our mass measurement with 6% uncertainties provides an important new constraint on the composition and internal structure of B-type asteroids. Combined with an IRAS size measurement, the mass yields a bulk density of 1570 ± 500 kg m^{-3}. This density admits an ice-to-rock mass ratio in the range 0-80%, depending on the porosity of the asteroid. Our density determination is significantly lower than previous estimates for the B-type asteroid (2) Pallas, which may be related to different porosities.

We thank referee W. Merline for insightful comments and F. Selman, C. Lidman, and N. Ageorges at the VLT for assistance with the observations. We are also grateful for the allocation of telescope time for follow-up observations, without which this binary could not have been fully characterized. PMR was supported by Center of Excellence in Astrophysics and Associated Technologies (PFB 06), FONDAP 15010003, and Fondecyt grant 11080271. JLM was supported by NASA Planetary Astronomy grant NNX07AK68G/NNX09AQ68G.

REFERENCES

V. Benishek. CCD Photometry of Seven Asteroids at the Belgrade Astronomical Observatory. *Minor Planet Bulletin*, 35:28–30, March 2008.

D. T. Britt, D. Yeomans, K. Housen, and G. Consolmagno. Asteroid Density, Porosity, and Structure. In W. F. Bottke, A. Cellino, P. Paolicchi, and R. P. Binzel, editors, *Asteroids III*, pages 485–500. Univ. of Arizona Press, 2002.

J. A. Burns. Two Bodies Are Better than One. *Science*, 297:942–943, August 2002.

S. J. Bus and R. P. Binzel. Phase II of the Small Main-Belt Asteroid Spectroscopic Survey A Feature-Based Taxonomy. *Icarus*, 158:146–177, July 2002.

B. Carry, C. Dumas, M. Kaasalainen, J. Berthier, W. J. Merline, S. Erard, A. Conrad, J. D. Drummond, D. Hestroffer, M. Fulchignoni, and T. Fusco. Physical properties of (2) Pallas. *Icarus*, 205:460–472, February 2010.

A. Conrad, B. Carry, J. D. Drummond, W. J. Merline, C. Dumas, W. M. Owen, C. R. Chapman, P. M. Tamblyn, R. W. Goodrich, and R. D. Campbell. Shape and Size of Asteroid (41) Daphne from AO Imaging. In *Bulletin of the American Astronomical Society*, volume 40 of *Bulletin of the American Astronomical Society*, September 2008.

D. D. Durda, W. F. Bottke, B. L. Enke, W. J. Merline, E. Asphaug, D. C. Richardson, and Z. M. Leinhardt. The formation of asteroid satellites in large impacts: results from numerical simulations. *Icarus*, 170:243–257, July 2004.

S. Foglia and G. Masi. New clusters for highly inclined main-belt asteroids. *Minor Planet Bulletin*, 31:100–102, December 2004.

R. Gil-Hutton. Identification of families among highly inclined asteroids. *Icarus*, 183:93–100, July 2006.

J. L. Hilton. Asteroids Masses and Densities. In W. F. Bottke, A. Cellino, P. Paolicchi, and R. P. Binzel, editors, *Asteroids III*, pages 103–112. Univ. of Arizona Press, 2002.

J. L. Hilton. US Naval Observatory Ephemerides of the Largest Asteroids. *AJ*, 117:1077–1086, February 1999.

T. V. Johnson and J. I. Lunine. Saturn's moon Phoebe as a captured body from the outer Solar System. *Nature*, 435:69–71, May 2005.

T. D. Jones, L. A. Lebofsky, J. S. Lewis, and M. S. Marley. The composition and origin of the C, P, and D asteroids - Water as a tracer of thermal evolution in the outer belt. *Icarus*, 88:172–192, November 1990.

A. S. Konopliv, C. F. Yoder, E. M. Standish, D.-N. Yuan, and W. L. Sjogren. A global solution for the Mars static and seasonal gravity, Mars orientation, Phobos and Deimos masses, and Mars ephemeris. *Icarus*, 182:23–50, May 2006.

H. P. Larson, M. A. Feierberg, and L. A. Lebofsky. The composition of asteroid 2 Pallas and its relation to primitive meteorites. *Icarus*, 56: 398–408, December 1983.

R. Lenzen, M. Hartung, W. Brandner, G. Finger, N. N. Hubin, F. Lacombe, A.-M. Lagrange, M. D. Lehnert, A. F. M. Moorwood, and D. Mouillet. NAOS-CONICA first on sky results in a variety of observing modes. In M. Iye and A. F. M. Moorwood, editors, *Instrument Design and Performance for Optical/Infrared Ground-based Telescopes. Edited by Iye, Masanori; Moorwood, Alan F. M. Proceedings of the SPIE, Volume 4841, pp. 944-952 (2003).*, volume 4841 of *Presented at the Society of Photo-Optical Instrumentation Engineers (SPIE) Conference*, pages 944–952, March 2003.

J. I. Lunine and W. C. Tittemore. Origins of outer-planet satellites. In *Protostars and Planets III*, pages 1149–1176, 1993.

J. L. Margot. Astronomy: Worlds of mutual motion. *Nature*, 416:694–695, April 2002.

J. L. Margot and M. E. Brown. A low density M-type asteroid in the main belt. *Science*, 300:1939–1942, 2003.

J. L. Margot, M. C. Nolan, L. A. M. Benner, S. J. Ostro, R. F. Jurgens, J. D. Giorgini, M. A. Slade, and D. B. Campbell. Binary asteroids in the near-earth object population. *Science*, 296:1445–8, 2002.

W. B. McKinnon, D. Prialnik, S. A. Stern, and A. Coradini. *Structure and Evolution of Kuiper Belt Objects and Dwarf Planets*, pages 213–241. 2008.

W. J. Merline, S. J. Weidenschilling, D. D. Durda, J. L. Margot, P. Pravec, and A.D. Storrs. Asteroids Do Have Satellites. In W. F. Bottke, A. Cellino, P. Paolicchi, and R. P. Binzel, editors, *Asteroids III*, pages 289–312. Univ. of Arizona Press, 2002.

G. Michalak. Determination of asteroid masses — I. (1) Ceres, (2) Pallas and (4) Vesta. *A&A*, 360:363–374, August 2000.

P. Michel, W. Benz, P. Tanga, and D. C. Richardson. Collisions and Gravitational Reaccumulation: Forming Asteroid Families and Satellites. *Science*, 294:1696–1700, November 2001.

K. S. Noll, W. M. Grundy, E. I. Chiang, J. L. Margot, and S. D. Kern. Binaries in the Kuiper Belt. In A. Barucci, M. Boehnhardt, D. Cruikshank, and A. Morbidelli, editors, *The Solar System Beyond Neptune*, pages 345–363. Univ. of Arizona Press, 2008.

S. J. Ostro, J. L. Margot, L. A. M. Benner, J. D. Giorgini, D. J. Scheeres, E. G. Fahnestock, S. B. Broschart, J. Bellerose, M. C. Nolan, C. Magri, P. Pravec, P. Scheirich, R. Rose, R. F. Jurgens, E. M. De Jong, and S. Suzuki. Radar Imaging of Binary Near-Earth Asteroid (66391) 1999 KW4. *Science*, 314:1276–1280, 2006.

J.-M. Petit, J. J. Kavelaars, B. J. Gladman, J. L. Margot, P. D. Nicholson, R. L. Jones, J. W. Parker, M. L. N. Ashby, A. Campo Bagatin, P. Benavidez, J. Coffey, P. Rousselot, O. Mousis, and P. A. Taylor. The Extreme Kuiper Belt Binary 2001 QW_{322}. *Science*, 322:432–, 2008.

P. Rojo and J. L. Margot. S/2007 (702) 1. *Central Bureau Electronic Telegrams*, 1016, August 2007.

G. Rousset, F. Lacombe, P. Puget, N. N. Hubin, E. Gendron, T. Fusco, R. Arsenault, J. Charton, P. Feautrier, P. Gigan, P. Y. Kern, A.-M. Lagrange, P.-Y. Madec, D. Mouillet, D. Rabaud, P. Rabou, E. Stadler, and G. Zins. NAOS, the first AO system of the VLT: on-sky performance. In P. L. Wizinowich and D. Bonaccini, editors, *Adaptive Optical System Technologies II. Edited by Wizinowich, Peter L.; Bonaccini, Domenico. Proceedings of the SPIE, Volume 4839, pp. 140-149 (2003).*, volume 4839 of *Presented at the Society of Photo-Optical Instrumentation Engineers (SPIE) Conference*, pages 140–149, February 2003.

K. Sato, M. Miyamoto, and M. E. Zolensky. Absorption bands near three micrometers in diffuse reflectance spectra of carbonaceous chondrites: Comparison with asteroids. *Meteoritics and Planetary Science*, 32: 503–507, July 1997.

B. E. Schmidt, P. C. Thomas, J. M. Bauer, J.-Y. Li, L. A. McFadden, M. J. Mutchler, S. C. Radcliffe, A. S. Rivkin, C. T. Russell, J. W. Parker, and S. A. Stern. The Shape and Surface Variation of 2 Pallas from the Hubble Space Telescope. *Science*, 326:275–, October 2009.

P. A. Taylor and J. L. Margot. Binary asteroid systems: Tidal ends states and estimates of material properties. *Icarus, submitted*, 2010.

E. F. Tedesco, P. V. Noah, M. Noah, and S. D. Price. The Supplemental IRAS Minor Planet Survey. *Astronomical Journal*, 123:1056–1085, February 2002.

S. J. Weidenschilling, P. Paolicchi, and V. Zappalà. Do asteroids have satellites? In R. P. Binzel, T. Gehrels, and M. S. Matthews, editors, *Asteroids II*, pages 643–660. University of Arizona Press, 1989.

B. Yang and D. Jewitt. Identification of Magnetite in B-type Asteroids. *AJ*, 140:692–698, September 2010.